Supernovae, Neutron Stars and Black Holes

Observations and their astrophysical interpretations of the explosive end stages of stellar evolution

PHYS 6210.01

Fall 2016

SN 1994D in NGC 4526

Credit: NASA, ESA, The Hubble Key Project Team, and The High-Z Supernova Search Team

Supernovae, Neutron Stars and Black Holes

Instructor: Prof. Norbert Bartel, PSE 331, bartel@yorku.ca www.yorku.ca/bartel
Course Number: PHYS 6210 1.0 F
Time/Location: W 16:00 to 17:00 ?

Textbooks:
Astrophysics, J. Irwin, Wiley, 2007
Theory of Stellar Structure and Evolution, 2nd edition, D. Prialnik, Cambridge University Press, 2009
Pulsar Astronomy, fourth edition, A. Lyne, F.Graham-Smith, Cambridge University Press, 2012
Introduction to High-Energy Astrophysics, S. Rosswog, M. Brueggen, Cambridge University Press, 2007
Supernovae and Gamma-Ray Bursters, K. Weiler, Lecture Notes in Physics, Springer, 2003

Course Contents:
1. Supernovae
   - 1.1 Classification and characteristics of supernovae
   - 1.2 Explosion process
   - 1.3 Shock front interaction with the Circum stellar medium
   - 1.4 Supernovae as distance indicators
2. Neutron stars
   - 2.1 Structure and magnetosphere of neutron stars
   - 2.2 Neutron star mass-radius relation for equations of state
   - 2.3 Characteristics of pulsars
   - 2.4 Pulsar emission mechanisms
   - 2.5 Pulsars as clocks for tests of general relativity
   - 2.6 Magnetars
   - 2.7 Gamma-ray bursts
3. Black holes
   - 3.1 Observational evidence for the existence of black holes
   - 3.2 The event horizon

Evaluation:
In-class quizzes: 15% of final mark
Homework: 35% of final mark
Project: 50% of final mark

Office hours: P331, MW 14:00-14:45

Rationale

- A supernova, the explosion of a star, is one of the most energetic single events in the universe. The burst of radiation released is so enormous that it can outshine an entire galaxy. During the explosion process most elements in the universe are created allowing the evolution of life.
- Neutron stars and black holes are the remnants of the explosion and provide us with examples to study fundamental aspects of matter, space and time.
- This specialized course is unique in focusing on the catastrophic end cycle of stars and relating it to our understanding of some of the central issues of physics.

1. Supernovae

1.1 Classification and characteristics of supernovae

Supernova nomenclature

- New supernova discovery reported to the International Astronomical Union's Central Bureau for Astronomical Telegrams (CBAT)
- It gives the supernova a name, SN is the marker, followed by the year of discovery, suffixed with a 1 or 2-letter designation.
- The first 26 supernovae in a year get a capital letter (A-Z). Following supernovae get a pair of small letters starting with aa, ab, etc.
- Every year 100's of supernovae are discovered.
- Since 2015 CBAT has scaled back assigning designations of supernovae because there are so many now.

Historical supernovae

- **Year Date Con RA Dec mag Comment/SNR**
- 185 AD Cen 14:43.1 -62:28 -2 (-6 mag acc. to Sky Catalog 2000)
- SNR: G315.4-2.3/RCW 86
- 386 Sgr 18:11.5 -19:25 SNR: G11.2-0.3 (?)
- 393/396 Sco 17:14 -39.8 -3 3 radio sources candidates for SN SNR: G347.3-0.5 (?)
- 1006 Apr 30 Lup 15:02.8 -41:57 -9+-1 SNR: PKS 1459-41
- 1054 Jul 4 Tau 05:34.5 +22:01 -6 M1 (Crab Nebula)
- 1181 Aug 6 Cas 02:05.6 +64:49 -1 3C 58
- 1572 Nov 6 Cas 00:25.3 +64:09 -4 Tycho
- 1604 Oct 9 Oph 17:30.6 -21:29 -3 Kepler
- 1680? 1667? Cas 23:23.4 +58:50 +6? Cas A SN

http://messier.seds.org/more/mw_sn.html

Figure 13-13
Discovering the Universe, Eighth Edition

Crab Nebula

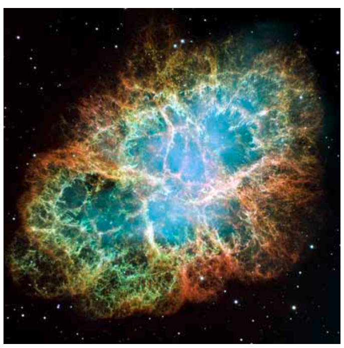

Tycho SNR

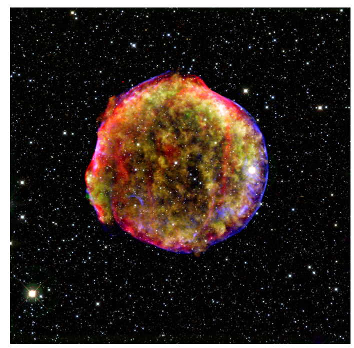

Cas A

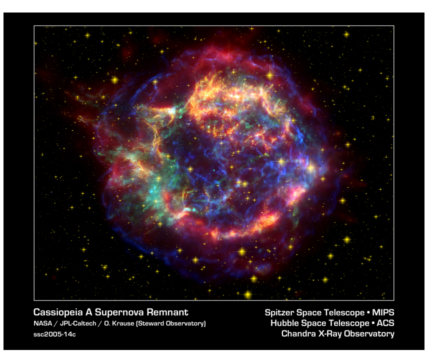

Light curve of a supernova (Type Ia)

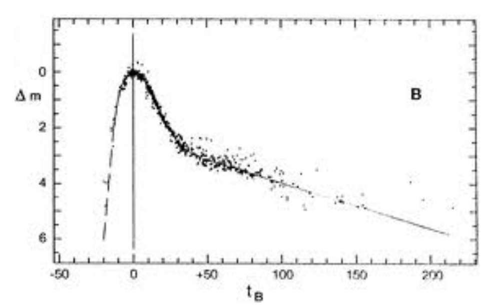

Stages of the light curve of a SN

- Energy is deposited through radioactive decay of Ni and Co into ejecta: $^{56}Ni + e \Rightarrow {}^{56}Co + \nu + \gamma$,
  $^{56}Co + e \Rightarrow {}^{56}Fe + \nu + \gamma$,
  $^{56}Co \Rightarrow {}^{56}Fe + e^{+} + \nu + \gamma$,
- The ejecta of the SN form an opaque sphere➔ luminosity is still low and given by L propto R^2T^4
- The sphere expands rapidly due to conversion of radiation into E_{kin} of the expanding sphere, and L increases rapidly.
- After some time the sphere becomes optically thin and L peaks.
- Then L is given by the exponential decay of ^{56}Ni and ^{56}Co

- Supernovae have been observed since ancient time but it was not known what supernovae were. Detailed modern observations of the lightcurves and the spectra revealed specific characteristics but also differences between the supernovae.
- A classification of supernovae was first proposed by Minkowsky (1941). He distinguished supernovae on the basis of whether H was not present or present in the spectra and introduced **Type I** and **Type II** supernovae, respectively.
- Zwicky (1965) introduced three more classes Type III, IV and V, but they are now all included in Type II supernovae.

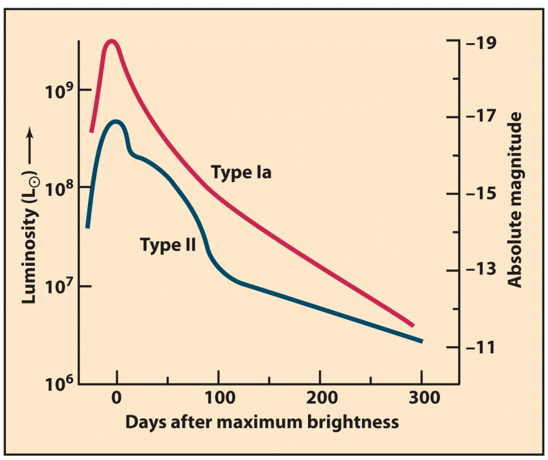

Figure 13-9
Discovering the Universe, Eighth Edition
© 2008 W.H. Freeman and Company

Two principally different kinds of SNe

- Thermonuclear detonation of a white dwarf (WD) in a binary system
  - WD accretes material from sun-like or giant companion, reaches Chandrasekhar limit of 1.4 M_{sol} and detonates

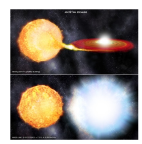

http://www.astronomynow.com/news/n1002/18darkenergy/accretion.jpg

  - WD cannibalizes second WD and detonates

- Core collapse of a massive star

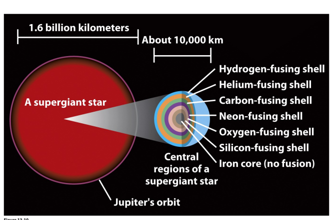

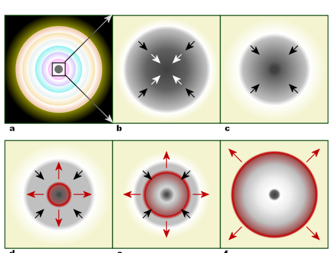

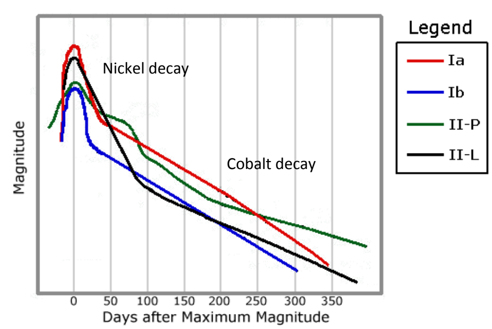

(adapted from Qing Zhang's "Introduction to Supernovae")

Type I:

In 1986 and 1987 it was noticed that some Type Ia's were peculiar. They had no SiII in their spectra. And of these some had HeI lines and others not.

That led to the naming of:

Type Ia (SiII present) and

Type Ib (no SiII but HeI present) and

Type Ic (no SiII and no HeI present).

- Type II: There is a wide variety of Type II supernovae. Four subclasses have been established, **Types IIP, IIL, IIn and IIb.** In addition there are peculiar supernovae that do not fit into these classes easily.
- **Type IIP (plateau)** and
- **Type IIL (linear)**

are the normal Type II's. Barbon, Ciatti and Rosino (1979) made the distinction on the basis of the lightcurves. They found lightcurves with a plateau (P) and then those with a linear uninterrupted decline (L). Schlegel (1990) classified Type II SN with narrow line emissions (~1000 km/s) as

- **Type IIn with "n" for narrow.**

Then there are

- **Type IIb SNe.**

They are characterized by having spectra at early times similar to those of Type II (prominent H lines) and then change into ones with spectra similar to Type Ib SNe. A prominent example is SN 1993J.

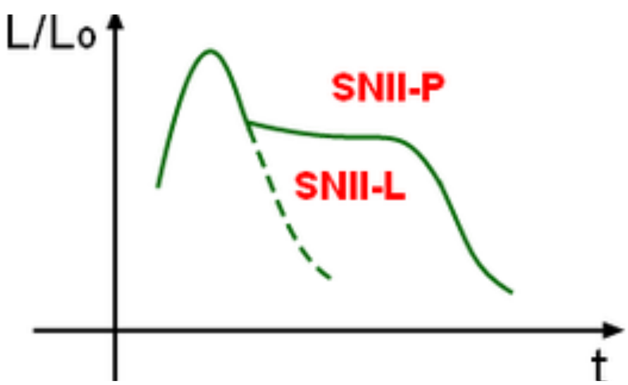

Classification scheme of non-peculiar SNe:

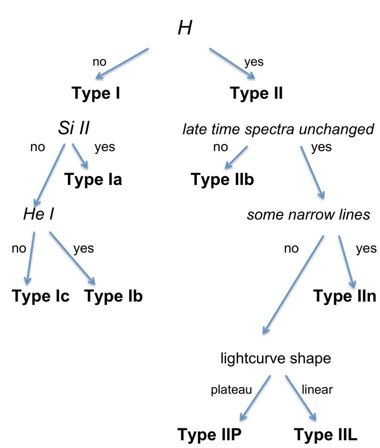

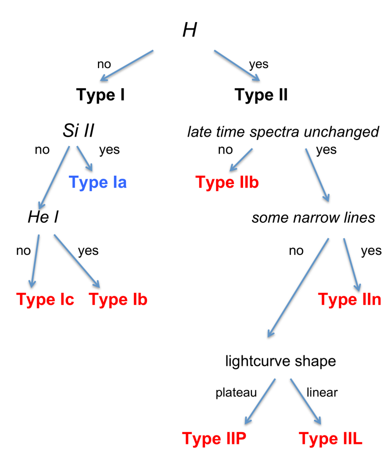

Blue: Detonation or deflagration of an accreting white dwarf
Red: Core collapse of a massive progenitor

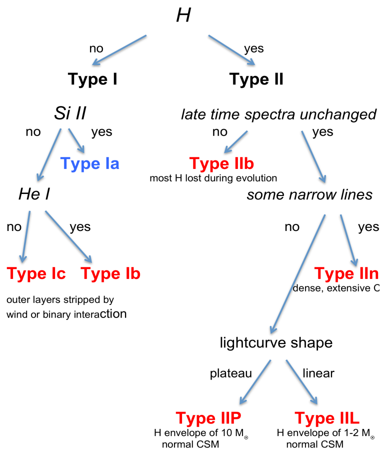

Classification of Supernovae 23

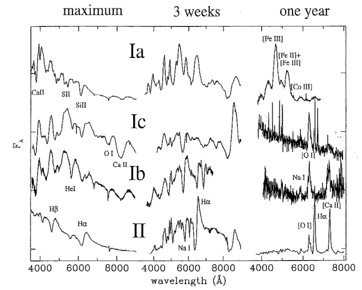

Fig. 2. The spectra of the main SN types at maximum, three weeks, and one year after maximum. The representative spectra are those of SN1996X for type Ia [109], of SN1994I (left and center) [35] and SN1997B (right) for type Ic, of SN1999dn (left and center) and SN1990I (right) for type Ib, and of SN1987A [99] for type II. At late times (especially in the case of the type Ic SN1997B the contamination from the host galaxy is evident as an underlying continuum plus unresolved emission lines. In all figures of this paper the spectra have been transformed to the parent galaxy rest frame.

P-Cygni profile

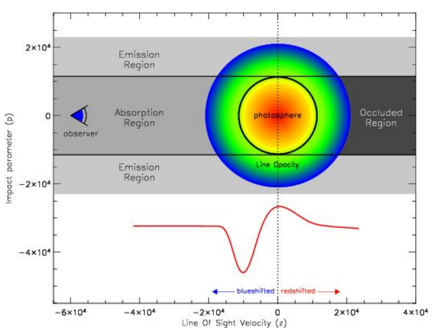

26 Massimo Turatto

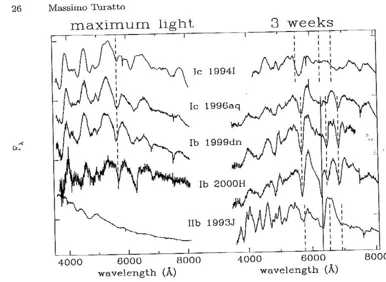

Fig. 3. Comparison among the spectra of SNe reported as type Ib/c in the Asiago SN Catalogue [8] (left: at maximum light; right: 3 weeks later). In addition to the spectra of SN1994I (SNIc) and SN1999dn (SNIb) shown in Fig. 2, the spectra of SN1996aq (SNIc), SN2000H (SNIb) [22] and SN1993J (SNIIb) [7] are displayed. With the exception of SN1993J, the spectra at maximum are rather similar. For reference the position of He I λ5876 (blueshifted by 10,500 km s^{-1}) is marked with a dashed vertical line. The dashed lines on the right indicate the positions of He I $\lambda\lambda$ 5876, 6678 and 7065 (blueshifted by 16,900 km s^{-1} for SN1994I, 6,000 km s^{-1} for SN1993J and 9,000 km s^{-1} for other objects). Hα (solid line, blueshifted by 11,000 km s^{-1}) is also shown. While He I lines in SN1994I are detectable only through a detailed analysis, they are prominent in the spectra of SN1996aq, which should be reclassified as a SNIb.

SN characteristics

Type 1A

- No H in spectrum
- Thermonuclear expl. of WD
- No compact remnant
- E_{kin} ~ 10^{51} erg
- V_{ejecta} ~ 5000 to 30,000 km/s
- No neutrino burst
- E_{opt} ~ 10^{49} erg
- L_{max} ~ 10^{43} erg (10 d)
- Lightcurve tail from ^{56}Co
- Occurs 1/300 yr in Galaxy
- Produces 2/3 of Fe in Galaxy
- Occurs in spirals and ellipticals

Type II

- H in spectrum
- Core collapse of M>8 M_{sol}
- NS or BH
- E_{kin} ~ 10^{51} erg
- V_{ejecta} ~ 2000 to 30,000 km/s
- Neutrino burst, 10^{53} erg
- E_{opt} ~ 10^{49} erg
- L_{max} ~ 2x10^{42} erg (100 d)
- Lightcurve tail from ^{56}Co
- Occurs 1/50 yr in Galaxy
- Produces 1/3 of Fe in Galaxy
- Occurs in spirals

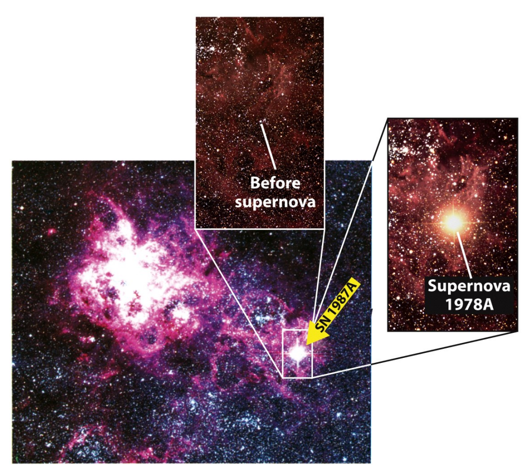

Figure 13-16
Discovering the Universe, Eighth Edition

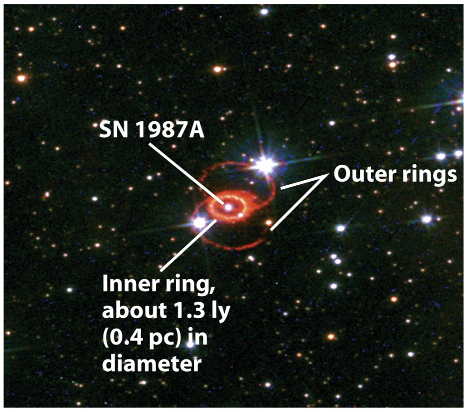

Supernova 1987A seen in 1996

Figure 13-17a
Discovering the Universe, Eighth Edition

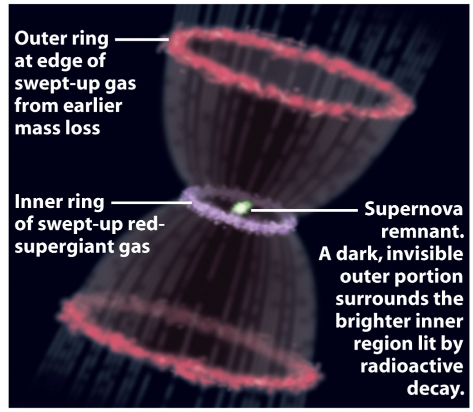

An explanation of the rings

Figure 13-17b
Discovering the Universe, Eighth Edition

1.2 Explosion processes

- There are two principally different explosion processes:
  thermonuclear explosion and explosion after core-collapse

  In each case, the details of the explosion processes are unknown. However models exist and scenarios are discussed.

Thermonuclear explosion

- All SNeType Ia undergo thermonuclear explosions.
- Thermonuclear explosions originate from white dwarfs in binary or triple systems.
- WD have masses of $0.2<M_{WD}<1.35\ M_\odot$ with a peak in the distribution of $0.6\ M_\odot$
- Most white dwarfs ($M>0.45\ M_\odot$) are carbon-oxygen stars. Therefore no H in spectra of SN Ia's. Gravitational inbound pressure balances electron degeneracy pressure, independent of T.

The most favoured model is the carbon ignition model at the Chandrasekhar mass

- Carbon ignites and fuses into heavier elements in the center of the WD when M_{WD} gets close to 1.4 M_{sol} (Chandrasekhar limit).
- ➔$E=10^{51}$ erg release can account for E_{kin} of ejecta with 5000 to 20000 km/s and for mass of ^{56}Ni to power light curve.
- ➔ Explosion always occurs at Chandrasekhar mass and can account for observed homogeneity of light curves.
- BUT: hard to accrete enough mass to account for SN Ia frequency.
- BUT: evolution of accreting star is complicated

- Carbon ignition sets in at $T=10^9$ K. Carbon and oxygen burn to nickel and iron.
  Thermonuclear runaway starts and ignites the whole WD.
- Computation very difficult. Nuclear reactions happen in 1cm layer (the flame). Energy production rate ~ T^{12}
- Question: deflagation (flame slow moving) or
  detonation (flame ast moving)?

The companion star- two scenarios

- Single-degenerate scenario
  - H is transferred from an evolved star to a WD in a close binary system
  - When total WD mass reaches 1.4 M_{sol}, the WD explodes

BUT: one should detect at least a bit of H in spectra of SN Ia which is not done

BUT: accretion is complicated

Single degenerate progenitors

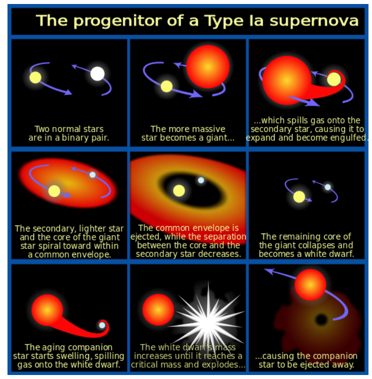

NASA, ESA and Feild

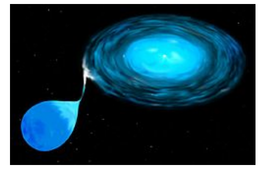

NASA

The companion star- two scenarios

- Double-degenerate scenario
  - A double WD system looses energy through gravitational wave emisson
  - WD's slowly spiral into each other. WD are the most common stars in the Universe and binary systems are also very common. A good fraction of all double WD's should be able to spiral into each other within 10 Bill years. That would be in accord with SN Ia frequency.
  - No H is expected in spectra
  - Explosion to occur at 1.4 M_{sol}

BUT: not clear whether collision leads to explosion. Ignition may start far from the center ➔ accretion induced collapse.

Collision of two White Dwarfs

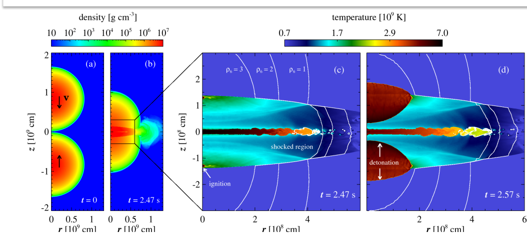

Kushnir et al. 2013

Core collapse explosion

- All SNe other than Type Ia undergo core-collapse explosions.
- Core-collapse explosions originate from massive evolved stars
- When a star has > 8M_{sol} it can burn fusion products all the way to Fe. In its very core it consists of onion-like layers of fusing elements.
- Most white dwarfs (M>0.45 $M_{\odot}$) are carbon-oxygen stars. Therefore no H in spectra of SN Ia's. Gravitational inbound pressure balances electron degeneracy pressure, independent of T.

Onion-like layers of a massive evolved star just before core-collapse

Star is stabilized by electron degeneracy pressure in core

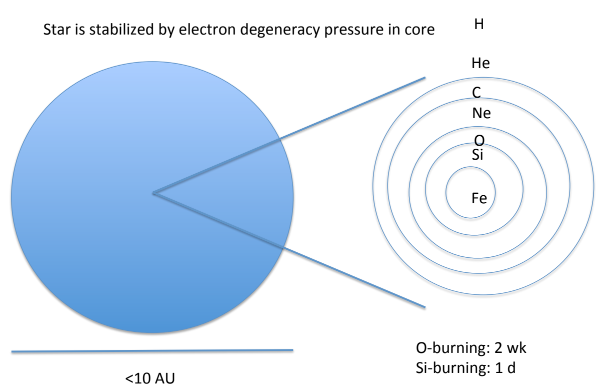

Fe as the most stable element

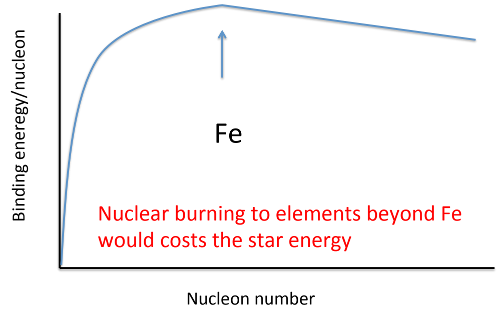

Core-collapse scenario

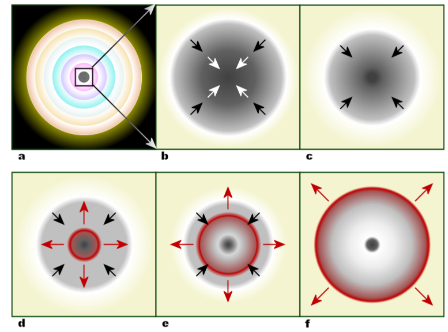

(a) A massive, evolved star has onion-layered shells of elements undergoing fusion. An inert iron core is formed from the fusion of Silicon in the inner-most shell. (b) This iron core reaches Chandrasekhar-mass and starts to collapse, with the outer core (black arrows) moving at supersonic velocity (shocked) while the denser inner core (white arrows) travel sub-sonically; (c) The inner core compresses into neutrons and the gravitational energy is converted into neutrinos. (d) The infalling material bounces off the nucleus and forms an outward-propagating shock wave (red). (e) The shock begins to stall as nuclear processes drain energy away, but it is re-invigorated by interaction with neutrinos. (f) The material outside the inner core is ejected, leaving behind only a degenerate remnant. (R. J. Hall)

Nuclear processes

- Typical processes:
  - photodisintegration

    $\gamma + {}^{56}Fe \Leftrightarrow 13\alpha + 4n$

    process costs energy, core collapses faster. That leads to higher densities which leads to

  - Electron captures

    $e^- + p \Rightarrow n + \nu_e$ and also on nuclei ➔ that reduces electron degeneracy pressure

1.2.2. Explosion following core collapse

- When the collapse leads to nuclear densities in the core of 3×10^{14} g cm^{-3} the nuclei are so densely packed together that the strong force becomes repulsive (r<0.7 fm). Collapse is stopped at about 20-30 km from center, material bounces back and causes an out-moving shock wave ➔ it should lead to explosion.

BUT: No simulation has yet produced an explosion

What could help explosion simulations?

Neutrinos seem to play a big role.

$E_{gravitational\text{-}binding} = 3 \times 10^{53}$ erg

$E_{kin} = 1 \times 10^{51}$ erg (shock)

It seems that some of the neutrinos' energy is deposited into the layers of the massive star and drives the explosion. Perhaps asymmetric explosions and magnetic fields are necessary to invoke tomake the star explode.

Neutrino burst detected from core-collapse SN 1987A

Confirmation that our basic understanding of core-collapse is right

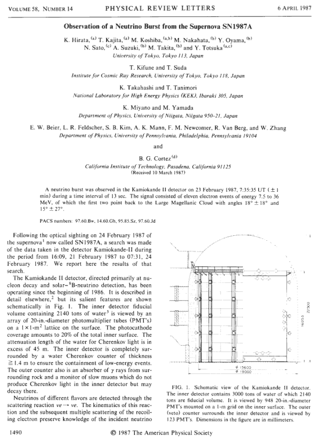
Volume 58, Number 14 PHYSICAL REVIEW LETTERS 6 April 1987

Observation of a Neutrino Burst from the Supernova SN1987A

K. Hirata,[a] T. Kajita,[a] M. Koshiba,[a,b] M. Nakahata,[b] Y. Oyama,[b] N. Sato,[c] A. Suzuki,[b] M. Takita,[b] and Y. Totsuka[a,c]
University of Tokyo, Tokyo 113, Japan

T. Kifune and T. Suda
Institute for Cosmic Ray Research, University of Tokyo, Tokyo 118, Japan

K. Takahashi and T. Tanimori
National Laboratory for High Energy Physics (KEK), Ibaraki 305, Japan

K. Miyano and M. Yamada
Department of Physics, University of Niigata, Niigata 950-21, Japan

E. W. Beier, L. R. Feldscher, S. B. Kim, A. K. Mann, F. M. Newcomer, R. Van Berg, and W. Zhang
Department of Physics, University of Pennsylvania, Philadelphia, Pennsylvania 19104

and

B. G. Cortez[d]
California Institute of Technology, Pasadena, California 91125
(Received 10 March 1987)

A neutrino burst was observed in the Kamiokande II detector on 23 February 1987, 7:35:35 UT (±1 min) during a time interval of 13 sec. The signal consisted of eleven electron events of energy 7.5 to 36 MeV, of which the first two point back to the Large Magellanic Cloud with angles 18° ± 18° and 15° ± 27°.

PACS numbers: 97.60.Bw, 14.60.Gh, 95.85.Sz, 97.60.Jd

Following the optical sighting on 24 February 1987 of the supernova[1] now called SN1987A, a search was made of the data taken in the detector Kamiokande-II during the period from 16:09, 21 February 1987 to 07:31, 24 February 1987. We report here the results of that search.

The Kamiokande II detector, directed primarily at nucleon decay and solar-^{8}B-neutrino detection, has been operating since the beginning of 1986. It is described in detail elsewhere,[2] but its salient features are shown schematically in Fig. 1. The inner detector fiducial volume containing 2140 tons of water[3] is viewed by an array of 20-in.-diameter photomultiplier tubes (PMT's) on a 1×1-m^2 lattice on the surface. The photocathode coverage amounts to 20% of the total inner surface. The attenuation length of the water for Cherenkov light is in excess of 45 m. The inner detector is completely surrounded by a water Cherenkov counter of thickness ≧1.4 m to ensure the containment of low-energy events. The outer counter also is an absorber of γ rays from surrounding rock and a monitor of slow muons which do not produce Cherenkov light in the inner detector but may decay there.

Neutrinos of different flavors are detected through the scattering reaction $\nu e \to \nu e$. The kinematics of this reaction and the subsequent multiple scattering of the recoiling electron preserve knowledge of the incident neutrino

FIG. 1. Schematic view of the Kamiokande II detector. The inner detector contains 3000 tons of water of which 2140 tons are fiducial volume. It is viewed by 948 20-in.-diameter PMT's mounted on a 1-m grid on the inner surface. The outer (veto) counter surrounds the inner detector and is viewed by 123 PMT's. Dimensions in the figure are in millimeters.

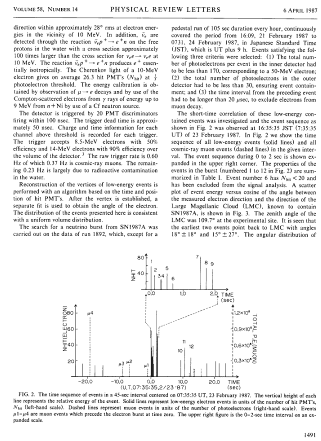

direction within approximately 28° rms at electron energies in the vicinity of 10 MeV. In addition, $\bar{\nu}_e$ are detected through the reaction $\bar{\nu}_e p^+ \to e^+ n$ on the free protons in the water with a cross section approximately 100 times larger than the cross section for $\nu_e e \to \nu_e e$ at 10 MeV. The reaction $\bar{\nu}_e p^+ \to e^+ n$ produces e^+ essentially isotropically. The Cherenkov light of a 10-MeV electron gives on average 26.3 hit PMT's (N_{hit}) at $\frac{1}{3}$ photoelectron threshold. The energy calibration is obtained by observation of $\mu \to e$ decays and by use of the Compton-scattered electrons from γ rays of energy up to 9 MeV from n+Ni by use of a Cf neutron source.

The detector is triggered by 20 PMT discriminators firing within 100 nsec. The trigger dead time is approximately 50 nsec. Charge and time information for each channel above threshold is recorded for each trigger. The trigger accepts 8.5-MeV electrons with 50% efficiency and 14-MeV electrons with 90% efficiency over the volume of the detector.[3] The raw trigger rate is 0.60 Hz of which 0.37 Hz is cosmic-ray muons. The remaining 0.23 Hz is largely due to radioactive contamination in the water.

Reconstruction of the vertices of low-energy events is performed with an algorithm based on the time and position of hit PMT's. After the vertex is established, a separate fit is used to obtain the angle of the electron. The distribution of the events presented here is consistent with a uniform volume distribution.

The search for a neutrino burst from SN1987A was carried out on the data of run 1892, which, except for a pedestal run of 105 sec duration every hour, continuously covered the period from 16:09, 21 February 1987 to 0731, 24 February 1987, in Japanese Standard Time (JST), which is UT plus 9 h. Events satisfying the following three criteria were selected: (1) The total number of photoelectrons per event in the inner detector had to be less than 170, corresponding to a 50-MeV electron; (2) the total number of photoelectrons in the outer detector had to be less than 30, ensuring event containment; and (3) the time interval from the preceding event had to be longer than 20 μsec, to exclude electrons from muon decay.

The short-time correlation of these low-energy contained events was investigated and the event sequence as shown in Fig. 2 was observed at 16:35:35 JST (7:35:35 UT) of 23 February 1987. In Fig. 2 we show the time sequence of all low-energy events (solid lines) and all cosmic-ray muon events (dashed lines) in the given interval. The event sequence during 0 to 2 sec is shown expanded in the upper right corner. The properties of the events in the burst (numbered 1 to 12 in Fig. 2) are summarized in Table I. Event number 6 has $N_{hit} < 20$ and has been excluded from the signal analysis. A scatter plot of event energy versus cosine of the angle between the measured electron direction and the direction of the Large Magellanic Cloud (LMC), known to contain SN1987A, is shown in Fig. 3. The zenith angle of the LMC was 109.7° at the experimental site. It is seen that the earliest two events point back to LMC with angles 18° ± 18° and 15° ± 27°. The angular distribution of

FIG. 2. The time sequence of events in a 45-sec interval centered on 07:35:35 UT, 23 February 1987. The vertical height of each line represents the relative energy of the event. Solid lines represent low-energy electron events in units of the number of hit PMT's, N_{hit} (left-hand scale). Dashed lines represent muon events in units of the number of photoelectrons (right-hand scale). Events $\mu1$–$\mu4$ are muon events which precede the electron burst at time zero. The upper right figure is the 0–2-sec time interval on an expanded scale.

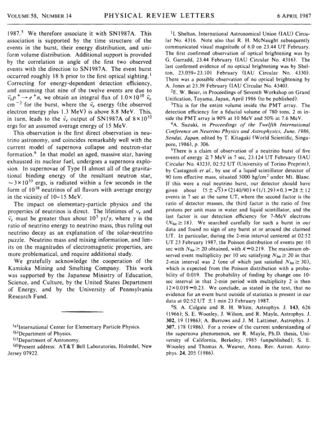

1.3. Interaction with the circumstellar medium

- Only massive progenitor stars have a history of loosing mass at their end stages of life.
- Only core-collapse SNe experience interaction of their shock fronts with the circumstellar medium (CSM).
- SN Type Ia's progenitors are WD which are the remnants of low-mass stars which experienced the planetary nebula phase a long time ago. Usually, there is no material left from that phase with which the shock front of the SN could interact.

Lit: Chevalier, Fransson 2003 in Supernovae and Gamma-ray bursters

The ejecta

- As soon as the shock breaks out of the surface of the exploding star it starts to interact with the CSM.
- The ejecta are described analytically by the density profile with an exponent n. The profile is assumed to be constant up to r_0 and then to fall off sharply:

$$\rho_{ej} = \rho_0 \left(\frac{t}{t_0}\right)^{-3} \left(\frac{r}{r}\right)^{-n}$$

$$r_0 = V_0 t_0$$

$$\rho_{ej} \propto t^{n-3} r^{-n}$$

- There are analytical limits to n: n_{max} =10-12
- For SN 1987A: n=8 to 9
- There is also a lower limit to n: n_{min} = 5

- For thermonuclear explosions, the ejecta profile is different since the explosion does not originate in the center but at locations where the flame burns through the star.

The CSM

- The CSM is generated by a wind from the progenitor, thousands of years before the star died. The wind is characterized by the mass loss, typically 10^{-6} to 10^{-4} M_{sol} yr^{-1} and by the wind velocity, w, typically 10 km s^{-1}.
- The CSM is also described analytically by a density profile with a power law,

$$\rho_{CSM} = \frac{\dot{M}}{4\pi w r^{s}}$$ with s=2 for constant mass loss.

VY Canis Majoris, the biggest star we know of

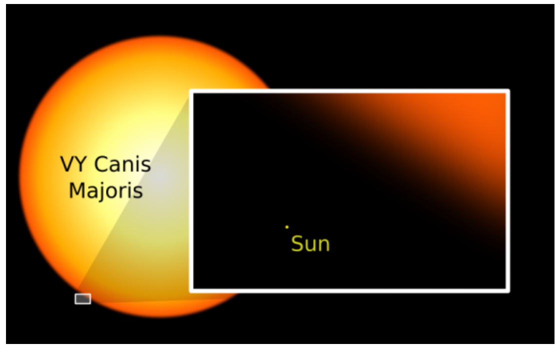

VY CMa

P_{csm} propto $(1/r^2)$

Hydrodynamics

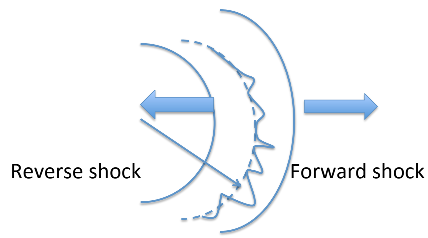

Contact discontinuity with Rayleigh Taylor instabilities

- It can be shown that the radius of the contact discontinuity is :
- ρ_0, t_0, V_0 :const

$$R_s(t) = \left[\frac{(n-4)(n-3)\dot{M}}{8\pi\rho_0 t_0^3 V_0^n w}\right]^{n-s} t^{\frac{n-3}{n-s}}$$

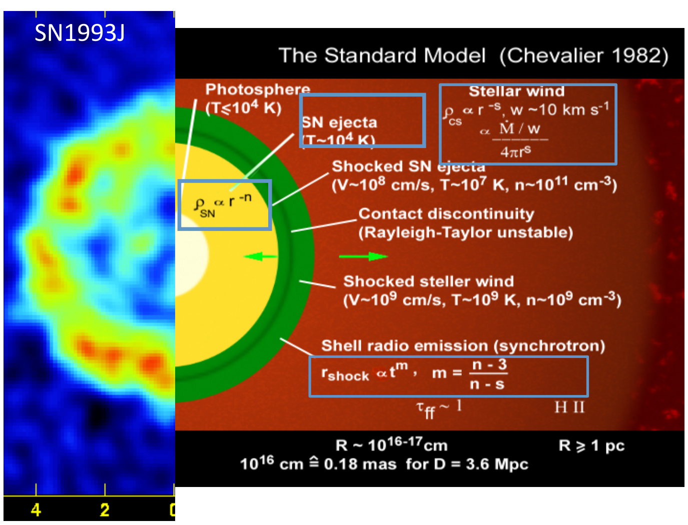

SN observations with VLBI

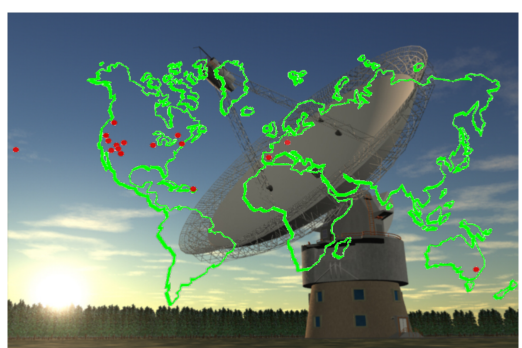

VLBI array

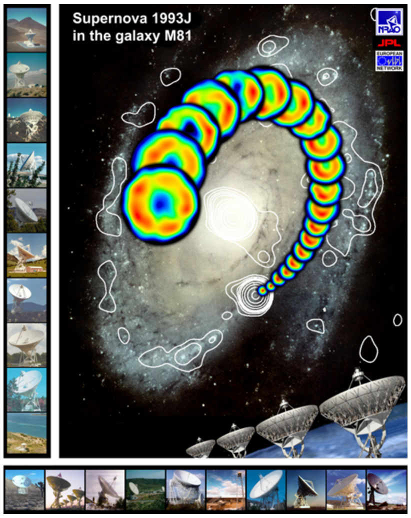

SN1993J
expansion and deceleration

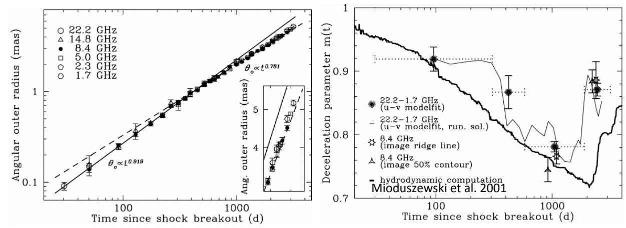

Deceleration changes with time:
n➔ determinable: very steep first, n~12, than flatter with time, n~6-7.

Bartel et al. 2002

Evolution of SN1993J

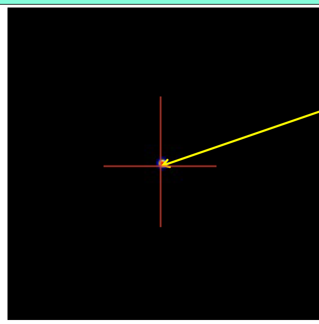

Position of Explosion Center known within 45µas (160AU).
--
Center of SN stable within 9 µas / yr
-

from t = 50d (r=200 AU) to t = 17 yr (r=34,000 AU)

Free download: www.yorku.ca/bartel

Evolution of SN1986J

NGC891

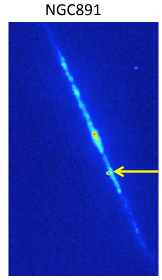

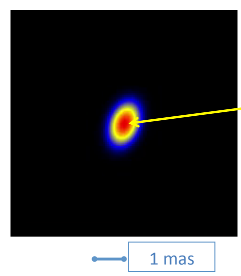

Youngest Neutron Star or Black Hole with 200 L_{Crab}?

Or dense shell condensation?

from t = 3 yr to t = 25 yr

Density ~20 times higher than that of northeastern condenstion, and located in forground on line of sight to center.

1.4 Supernovae as distance indicators

- Expanding photosphere method (EPM)
- Expanding shock front method (ESM)
- SNIa as standard candles

- The first two methods work on determining the distance, D, directly from the linear, R, and angular, Θ, radii:

$$D = \frac{R}{\theta}$$

- The third method works on comparing the luminosity with the brightness.

Lit: Chevalier, Fransson 2003 in Supernovae and Gamma-ray bursters

Expanding photosphere method

EPS works on the basis that the radius, R =R_{ph}, of the supernova is determined through

$$R_{ph} = V_{ph}(t - t_0) + R_0$$

with V_{ph} :radial velocity determined from spectral lines

t-t_0 :time since shock breakout

R_0 : initial radius

- The angular radius is determined with the assumption that the supernova is optically thick in its interior and that therefore the supernova can be considered a black body.
- For a black body the luminosity of the supernova can be determined from the surface temperature, T:
- Where F is the flux in W/m^2 of the radiation leaving the surface

$$L = 4\pi R_{ph}^2 \sigma T^4$$
$$F = \sigma T^4$$
$$\sigma = 5.67 \bullet 10^{-8} W m^{-2} K^{-4}$$

Supernova as a black body

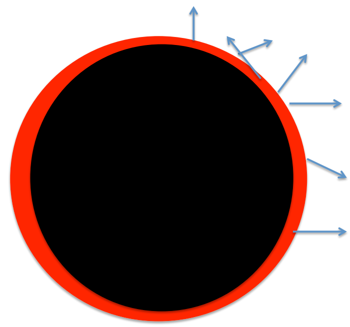

H gas is ionized. Opacity is high, no radiation gets out. Only radiation from a surface shell leaves the star. That radiation has an intensity almost completely given by the temperature of the gas in that shell. The temperature is 4000 to 6000K, Just enough for H to recombine and be optically thin. Further down in the interior all the H is ionized and radiation does not get out.

The spectral flux [W m^{-2} nm^{-1}] from the surface is determined by the Planck curve:

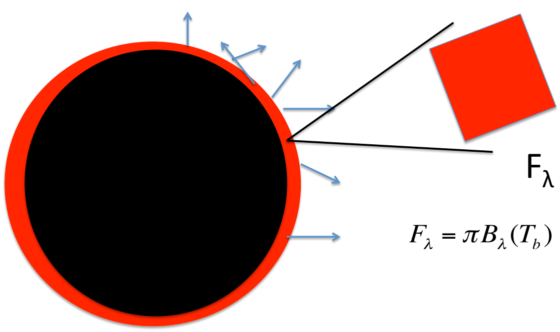

$$F_\lambda = \pi B_\lambda(T_b)$$

Planck curves

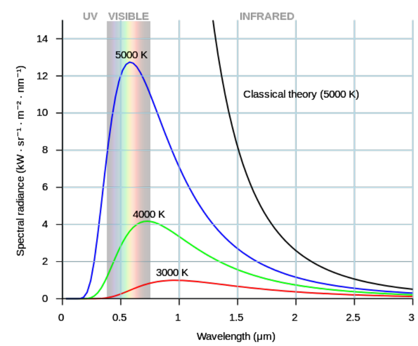

$$B_\lambda(T) = \frac{2hc^2}{\lambda^5} \frac{1}{e^{\frac{hc}{\lambda kT}} - 1}$$

- The observed flux is given by

$$F' = \frac{L}{4\pi D^2}$$
$$F' = \frac{R_{ph}^2}{D^2} F = \theta_{ph}^2 \sigma T^4$$

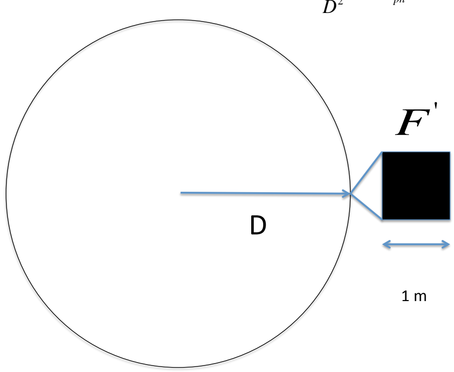

The observed spectral flux is given by:

$$F'_\lambda = \frac{R_{ph}^2}{D^2} F_\lambda$$
$$F'_\lambda = \frac{R_{ph}^2}{D^2} \pi B_\lambda(T_b)$$

- Now all parameters are measurable quantities and the angular radius is given by:

$$\theta_{ph} = \frac{R_{ph}}{D} = \sqrt{\frac{F'_\lambda}{\pi B_\lambda(T_b)}}$$

- With several measurements of T, R_{ph}, t and F'_λ we can fit the equation, $t = D\left(\frac{\theta_{ph}}{V_{ph}}\right) + t_0$ to the data and determine D and t_0. Further, $R_{ph}(t_0)=R_0$ can be determined as well.

- THE VERY YOUNG TYPE IA SUPERNOVA 2013DY: DISCOVERY, AND STRONG CARBON ABSORPTION IN EARLY-TIME SPECTRA
- WeiKang Zheng1,2, Jeffrey M. Silverman3,4, Alexei V. Filippenko1, Daniel Kasen5,6, Peter E. Nugent5,1, Melissa Graham1,7,8, Xiaofeng Wang9, Stefano Valenti7,8, Fabrizio Ciabattari10, Patrick L. Kelly1, Ori D. Fox1, Isaac Shivvers1, Kelsey I. Clubb1, S. Bradley Cenko11, Dave Balam12, D. Andrew Howell7,8, Eric Hsiao13,
- Weidong Li1,14, G. Howie Marion3,15, David Sand16, Jozsef Vinko17,3, J. Craig Wheeler3, and JuJia Zhang18,19
- Draft version October 22, 2013
- ABSTRACT
- The Type Ia supernova (SN Ia) 2013dy in NGC 7250 (d ≈ 13.7 Mpc) was discovered by the Lick Observatory Supernova Search. Combined with a prediscovery detection by the Italian Supernova Search Project, we are able to constrain the first-light time of SN 2013dy to be only 0.10 ± 0.05 d (2.4 ± 1.2 hr) before the first detection. This makes SN 2013dy the earliest known detection of an SN Ia**. We infer an upper limit on the radius of the progenitor star of R0 [?] 0.25 R⊙, consistent with that of a white dwarf.** The light curve exhibits a broken power law with exponents of 0.88 and then 1.80. A spectrum taken 1.63 d after first light reveals a C II absorption line comparable in strength to Si II. This is the strongest C II feature ever detected in a normal SN Ia, suggesting that the progenitor star had significant unburned material. The C II line in SN 2013dy weakens rapidly and is undetected in a spectrum 7 days later, indicating that C II is detectable for only a very short time in some SNe Ia. SN 2013dy reached a B-band maximum of MB = −18.72 ± 0.03 mag ~17.7 d after first light. Subject headings: supernovae: general — supernovae: individual (SN 2013dy)

Assumptions

- Spherical symmetry
- Free expansion
- Understanding of supernova photosphere

C

- Spectral flux densities are not given and are not measured directly. Instead the apparent magnitude is measured for a particular band.
- Particular bands are U, B, V for ultra violet, blue and visual. The band passes for these bands do not have a rectangular form but rather a distorted Gaussian form. The apparent magnitude is then a function of the integral of the observed spectral flux density times the band pass over frequency. Fortunately, these integrals are available on the web. So we can convert apparent magnitude into (effective) observed spectral flux density at the midpoint of the frequency range of the band pass and determine D, t_0, and R_0.

Johnson and Morgan UBV filter system transmission curves.

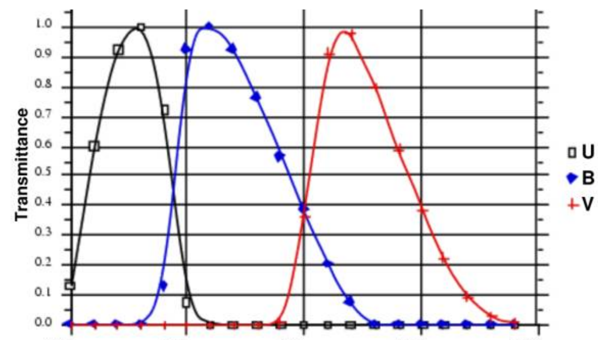

THE ASTROPHYSICAL JOURNAL, 395:366–386, 1992 August 20
© 1992. The American Astronomical Society. All rights reserved. Printed in U.S.A.

EXPANDING PHOTOSPHERES OF TYPE II SUPERNOVAE AND THE EXTRAGALACTIC DISTANCE SCALE[1]

BRIAN P. SCHMIDT AND ROBERT P. KIRSHNER[2]
Harvard-Smithsonian Center for Astrophysics, 60 Garden Street, Cambridge, MA 02138
AND
RONALD G. EASTMAN
Harvard-Smithsonian Center for Astrophysics; and Board of Studies in Astronomy and Astrophysics, Lick Observatory, University of California Santa Cruz, Santa Cruz, CA 95064
Received 1991 October 25; accepted 1992 February 25

ABSTRACT

We use the Expanding Photosphere Method to determine distances to 10 Type II supernovae. The effects of asymmetries, extinction, and flux dilution are explored. Using empirical evidence and time-dependent, spherical models which treat H and He in non–LTE, we show that blackbody corrections caused by flux dilution are small for Type II supernovae in the infrared, and in the optical when their color temperatures are less than 6000 K. The extinction to a Type II-P supernova can be estimated from its light curve: the uncertainty introduced into a distance measurement due to extinction is usually less than 10%. Correcting for extinction and flux dilution, we derive distances to 10 supernovae: SN 1968L, SN 1969L, SN 1970G, SN 1973R, SN 1979C, SN 1980K, SN 1987A, SN 1988A, SN 1990E, and SN 1990ae. The distance measurements span a wide range, 50 kpc to 120 Mpc, which is unique among the methods for establishing the extragalactic distance scale. The distances measured to SN 1970G in M101 and SN 1987A in the LMC are in good agreement with distances determined from Cepheid variable stars. Our distance to the Virgo Cluster, 22 ± 3 Mpc, is larger than recent distance estimates made using surface brightness fluctuations, planetary nebula luminosity functions, and the Tully-Fisher method. Using the distances determined from these Type II supernovae, we derive a value of $H_0 = 60 \pm 10$ km s^{-1} Mpc^{-1}. This value is subject to errors caused by local deviations in the Hubble flow but will soon be improved by applying the Expanding Photosphere Method to several distant Type II supernovae.

Subject headings: cosmology: observations — distance scale — supernovae: general

1. INTRODUCTION

The path to the extragalactic distance scale is long, complex, and pitted with traps for the unwary. Most distance indicators that are useful at the distance of the Virgo Cluster and beyond are calibrated with nearby galaxies whose distances have been [illegible]

The primitive form of EPM described by Kirshner & Kwan (1974) assumes that a SN II consists of a spherically symmetric expanding photosphere that radiates as a blackbody. If $z \ll 1$, [illegible]

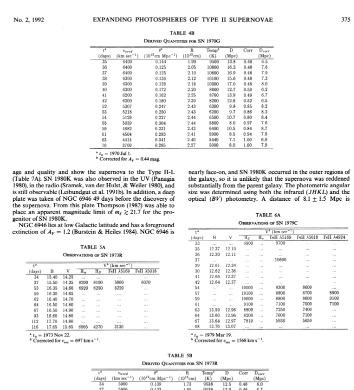

No. 2, 1992 EXPANDING PHOTOSPHERES OF TYPE II SUPERNOVAE 375

© American Astronomical Society • Provided by the NASA Astrophysics Data System

Expanding shock front method

$$D = \frac{R_o}{\theta_o}$$

- The radius is determined from the time of shock breakout and the maximum velocities of the H gas determined from the blue edge of the Hα lines. $R_o = v_{H\_max}(t - t_o)$
- The angular outer shell radius, Θ_o, is determined directly through VLBI measurements
- As an alternative: $D = \frac{\dot{R}_o}{\dot{\theta}_o}$

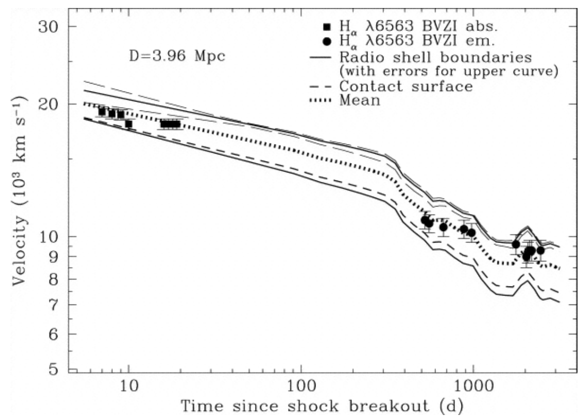

- The Astrophysical Journal, 668:924Y940, 2007 October 20

- SN 1993J VLBI. IV. A GEOMETRIC DISTANCE TO M81 WITH THE EXPANDING SHOCK FRONT METHOD
- N. Bartel and M. F. Bietenholz
- Department of Physics and Astronomy, York University, Toronto, ON M3J 1P3, Canada
- M. P. Rupen
- National Radio Astronomy Observatory, Socorro, NM 87801
- and
- V. V. Dwarkadas
- Department of Astronomy and Astrophysics, University of Chicago, Chicago, IL 60637
- Received 2007 January 8; accepted 2007 July 2 ABSTRACT
- We compare the angular expansion velocities, determined with VLBI, with the linear expansion velocities mea- sured from optical spectra for supernova 1993J in the galaxy M81, over the period from 7 days to ~9 yr after shock breakout, and estimate the distance to SN 1993J using the expanding shock front method (ESM). We find that the best distance estimate is obtained by fitting the angular velocity of a point halfway between the contact surface and outer shock front to the maximum observed hydrogen gas velocity. We obtain a direct, geometric, distance estimate for M81 of D 1⁄4 3:96 □ 0:05 □ 0:29 Mpc with statistical and systematic error contributions, respectively, which combine to a total standard error of □0.29 Mpc. The upper limit of 4.25 Mpc corresponds to the hydrogen gas with the highest ob- served velocity just reaching out to the contact surface a few days after shock breakout. The lower limit of 3.67 Mpc corresponds to this gas reaching as far out as the forward shock for the whole observing period, which would mean that Rayleigh-Taylor fingers have grown to the forward shock already a few days after shock breakout. Our distance estimate is 9% □ 13% larger than that of 3:63 □ 0:34 Mpc from the HST Key Project. The radio shell and the H□ absorbing and emitting gas are similarly decelerated on average, but the latter slightly less so than the former several years after shock breakout. This may indicate developing Rayleigh-Taylor fingers, extending progressively further into the shocked cir- cumstellar medium.
- Subject headinggs: radio continuum: general — supernovae: general — supernovae: individual (SN 1993J)

Assumptions

- Spherical symmetry (but symmetry on the sky can be determined directly through imaging
- Understanding the radio and optical line emitting regions

SNe Type Ia as standard candles

- This method is the most important one and won S. Perlmutter, B. Schmidt and A. Ries the 2011 Nobel Prize in Physics.
- In contrast to the former two methods, this method depends on a zero point calibration.
- Distances are determined via the distance modulus with m and M as apparent and absolute magnitudes:
- $m - M = 5\log_{10}(D[pc]) - 5$
- $D[pc] = 10^{0.2(m-M)+1}$

History-leading to the Nobel Prize in Physics in 2011

- SNIa have been used as distance indicators since 1968 (Kowal 1968)
- By~1990 it was recognized that the vast majority of SNIa's have similar light curve shapes, spectral time series and absolute magnitudes (ΔM_{max}<0.25) ➔ best known standard candles.
- When correlation between M_{max} and light curve decline was taken into account, (ΔM_{max}<0.20) .
- Multi-color light curve shape method: fit of light curves in all colors allowed correction for intervening dust (extinction) (Riess et al. 1996).
- Stretch method: All light curves could be matched by time stretching or contraction of a canonical light curve
- Now: ΔM_{max}<0.18, ➔ 6% distance error.

Obstacles to measuring luminosity distances with SNIa

- K-correction: The light curve is slightly wavelength dependent. Cosmological redshift shifts the spectrum of the light curve within the bands of the telescope. K-correction corrects for the shift. ~0.01 mag.
- Extinction: residual error 0.06 mag.
- Gravitational lensing: due to fluctuations in the gravitational potential the maximum of a light curve can be subject to slight variations. ~<0.02 mag
- Evolution: SNIa light curve shapes depend on the type of the host galaxy. SNIa in early type galaxies rise and fade in light more quickly than SNIa in late type galaxies (lots of star formation) ➔ metallicity effect.

Acceleration of the Universe

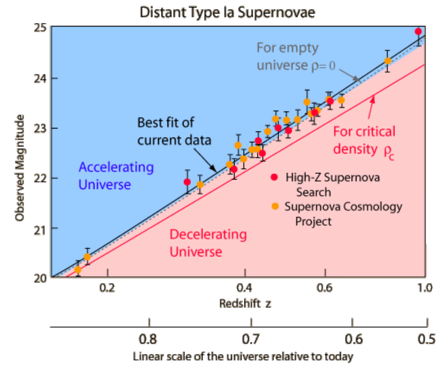

Perlmutter